AGU PUBLICATIONS

Geophysical Research Letters

RESEARCH LETTER
10.1002/2017GL073827

Key Points:
- Time-varying Lagrangian transport formulation in heterogeneous catchments leads to mean travel times that are not significantly biased to spatial aggregation
- There exists a characteristic spatial scale above which the aggregation of spatial heterogeneity does not influence the mean travel time
- The catchment characteristic scale at which aggregation effects vanish divided by the mean incremental area is on average independent of river network topology

Supporting Information:
- Supporting Information S1

Correspondence to:
M. Danesh-Yazdi,
dane0049@umn.edu

Citation:
Danesh-Yazdi, M., G. Botter, and E. Foufoula-Georgiou (2017), Time-variant Lagrangian transport formulation reduces aggregation bias of water and solute mean travel time in heterogeneous catchments, *Geophys. Res. Lett.*, *44*, doi:10.1002/2017GL073827.

Received 13 APR 2017
Accepted 28 APR 2017
Accepted article online 4 MAY 2017

Time-variant Lagrangian transport formulation reduces aggregation bias of water and solute mean travel time in heterogeneous catchments

Mohammad Danesh-Yazdi[1], Gianluca Botter[2], and Efi Foufoula-Georgiou[3]

[1]Department of Civil, Environmental, and Geo-Engineering, St. Anthony Falls Laboratory, and National Center for Earth-Surface Dynamics, University of Minnesota, Minneapolis, Minnesota, USA, [2]Dipartimento di Ingegneria Civile, Edile e Ambientale, Università degli studi di Padova, Padua, Italy, [3]Department of Civil and Environmental Engineering, University of California, Irvine, California, USA

Abstract Lack of hydro-bio-chemical data at subcatchment scales necessitates adopting an aggregated system approach for estimating water and solute transport properties, such as residence and travel time distributions, at the catchment scale. In this work, we show that within-catchment spatial heterogeneity, as expressed in spatially variable discharge-storage relationships, can be appropriately encapsulated within a lumped time-varying stochastic Lagrangian formulation of transport. This time (variability) for space (heterogeneity) substitution yields mean travel times (MTTs) that are not significantly biased to the aggregation of spatial heterogeneity. Despite the significant variability of MTT at small spatial scales, there exists a characteristic scale above which the MTT is not impacted by the aggregation of spatial heterogeneity. Extensive simulations of randomly generated river networks reveal that the ratio between the characteristic scale and the mean incremental area is on average independent of river network topology and the spatial arrangement of incremental areas.

Plain Language Summary The absence of rigorous data and theories for extrapolating information from the field to the larger scales necessitates developing reduced-complexity frameworks that are still able to explain the spatial heterogeneity and process complexity in real-world catchments. In this study, we examined the ability of the lumped stochastic Lagrangian formulation for water and solute transport in providing reliable estimates of the mean travel time (MTT) in spatially heterogeneous catchments. Via numerical simulations of heterogeneous catchments, we showed that a time-varying travel time distribution formulation results in MTTs that are not significantly biased to the aggregation of spatial heterogeneity under different age sampling assumptions. This finding reinforces the importance of such a time-variant lumped formalism to appropriately predict the catchment's mean transport time scales without the need to explicitly characterize and embed the small-scale spatial heterogeneity. We also showed that although significant variability of MTT exists at small spatial scales, there exists a characteristic spatial scale above which the MTT converges to a constant value not influenced by the aggregation of spatial heterogeneity. The above findings have practical implications pertaining to data measurements in the field and inferences that can be made on transport time scales and mixing processes across spatial scales.

1. Introduction

The residence and travel time of water in a catchment carry integral information about flow pathways and velocities, sources of water, and degree of mixing, together controlling chemical composition and biogeochemical cycling [e.g., *Hornberger et al.*, 2001; *Botter et al.*, 2009; *Soulsby et al.*, 2009; *Benettin et al.*, 2013a]. Reliable prediction of the fate of contaminants in response to loading reduction to meet water quality standards hinges on accurate estimation of water and solute travel time distributions (TTDs) [e.g., *Sanford and Pope*, 2013], typically relying on modeling. Although detailed transport models with a large number of parameters might explain some physical processes of interest at the field scale, provided that enough observations are available for attribution of cause and effect [e.g., *Woo and Kumar*, 2016], they are infeasible at the large watershed scale. How to upscale information from the field scale to the catchment scale is still a challenge both in terms of effective parameterizations and in using available observations [e.g., *Hrachowitz et al.*, 2013; *Birkel and Soulsby*, 2015]. Moreover, developing lumped system representations that allow for

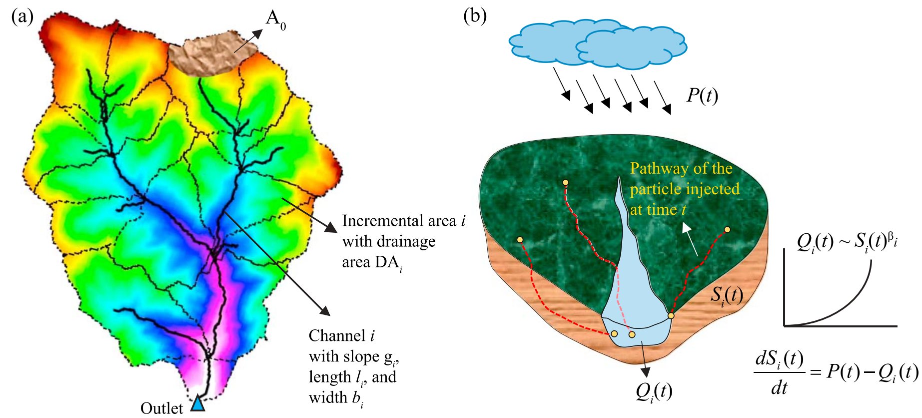

Figure 1. Schematic of a catchment decomposition into incremental areas (IAs), each IA represented by a single storage model. (a) A hypothetical catchment *w* composed of channels *i*, *i* = 1,..., *N*, each with incremental drainage area DA*i*. Each channel is characterized by its length, gradient, and width denoted by *li*, *gi*, and *bi*, respectively, and A_0 is the channel initiation area. (b) Illustration of a single storage model at which the mass balance holds between precipitation (*P*), soil storage (*Si*), and discharge (*Qi*). Evapotranspiration is ignored for simplicity.

accurate estimation of whole catchment behavior without explicitly incorporating the small-scale heterogeneity also remains a challenge [e.g., *Young*, 2003; *Kirchner*, 2006].

Several studies have utilized seasonal tracer cycles in precipitation and streamflow to infer a catchment TTD by treating the catchment as a lumped system and assuming a steady state predefined shape (e.g., exponential or gamma) for the underlying TTD [see *McGuire and McDonnell*, 2006, and reference therein]. Such a consideration is inconsistent with both temporal and within-catchment spatial variations of TTDs because (i) TTDs are nonstationary due to the temporal variability of hydrologic fluxes [e.g., *Rinaldo et al.*, 2011] and the fact that the temporal variation of their statistics might be slaved to the overall system dynamics [e.g., *Danesh-Yazdi et al.*, 2016] and (ii) even if time-invariant TTDs (e.g., exponential distribution in the simplest case) are assumed for the incremental areas (IAs) of a catchment, as the aggregation of IAs takes place, the shape of the combined TTD would be quite different from the TTDs of any of the individual IAs.

In this work, we seek to examine the ability of the theory of time-variant TTDs [*Botter et al.*, 2010, 2011; *van der Velde et al.*, 2012; *Benettin et al.*, 2015b; *Harman*, 2015] to accurately predict the catchment transport properties in the absence of within-catchment observations. In particular, this study explores the following questions: (1) Can a lumped system representation via the stochastic Lagrangian transport formulation, which does not demand explicit characterization of within-catchment spatial heterogeneity, properly capture the influence of this spatial heterogeneity into the transport time scales expressing the system storage and mixing? (2) What is the dependence of the TTD on the network-structured spatial heterogeneity as the hierarchical aggregation of IAs takes place? (3) Does a characteristic spatial scale exist above which the MTT becomes independent of the spatial heterogeneity of IAs? If so, what controls its magnitude?

2. Methods and Assumptions

2.1. Generation of Spatially Heterogeneous Catchments

Let w denote a catchment composed of two or more IA_i, $i = 1,\ldots, N$, that are connected via a river network topology with maximum Horton-Strahler order, Ω (Figure 1a). We use the Tokunaga self-similar (TSS) model to represent the river network topology; that is, we assume that $T_k = ac^{k-1}$ where T_k is the average number of branches of order j per branch of order $(j + k)$, and a and c are positive parameters (see, e.g., *Peckham* [1995a, 1995b] and *Zanardo et al.* [2013] for a review and extensive analysis of TSS trees in the context of river networks). Let l_i, g_i, and b_i represent the length, gradient, and width of the channel corresponding to IA_i, respectively. We assume that the drainage area of the IA_i, i.e., DA_i, follows an exponential distribution with mean λ, that is, $f(DA_i) \sim \exp(1/\lambda)$, and g_i and b_i are assumed to obey the typical scaling relationships for fluvial networks, i.e., $g_i \sim A_i^{-0.30}$ and $b_i \sim A_i^{0.35}$ [e.g., *Rodríguez-Iturbe and Rinaldo*, 2001], where A_i is the total upstream area of the outlet of the IA_i. If L_i is the length of the longest stream from the outlet of IA_i to its most upstream catchment divide and we assume Hack's law, i.e., $L_i \sim A_i^{0.55}$ [*Hack*, 1957], the channel length l_i can then be hierarchically computed through the river network. Using the above procedure, spatially heterogeneous catchments of arbitrary order can be generated.

2.2. Hydrologic Model

The flow through each IA_i is simulated using a single storage (reservoir) model (Figure 1b). Precipitation (P) is considered spatially uniform across all IA_i, evapotranspiration is ignored for simplicity, and the discharge (Q_i)-storage (S_i) relationship is assumed to be a power law with parameters K_i and β_i, i.e.,

$$Q_i(t) = K_i S_i(t)^{\beta i}. \tag{1}$$

Kirchner [2016b] proposed that the coefficient K in equation (1) can be parameterized by the exponent β and a storage value called "reference" storage, S_{ref}. Being much more meaningful and easier to interpret than K, the reference storage is a surrogate for the residual storage when β_i is significantly larger than 1 and represents the storage levels at which Q equals the long-term average input rate ($\overline{P}$), i.e., $\overline{P} = \mathrm{K}S_{\mathrm{ref}}^{\beta}$. As such, the mass balance for IA_i is written as

$$\frac{dS_i(t)}{dt} = P(t) - \overline{P}\left(\frac{S_i(t)}{S_{i,ref}}\right)^{\beta i}. \tag{2}$$

2.3. Time-Variant Travel Time Distribution (TTD) Analysis

The theory of time-variant TTD has been developed based on the Lagrangian representation of a catchment, where the water and solute particles are tracked along their spatially heterogeneous hydrologic pathways. The probability distribution of the particles' stochastic displacement is expressed by the Fokker-Planck equation [e.g., *Risken*, 1984], which is similar in form to the advection-dispersion model. Also, each particle contained within the catchment is labeled by its age or residence time (t_R) which is the difference between the current time and the time at which it entered the catchment, while the particle's travel time (t_T) is defined as the time between its entrance to and exit from the catchment. Therefore, the age of a particle evolves over time and coincides with its travel time only when the particle exits the catchment. In the same location at a given time, particles with different ages can be found and their distribution can be characterized by the mass age density function [*Ginn*, 1999]. The linkage between the displacement and the mass age distribution functions [*Benettin et al.*, 2013b] constitutes the basis for the master equation [*Botter et al.*, 2011], describing how the age distribution of the particles evolves over time both in the storage (as quantified by time-variant residence time distributions) and in the outflow (as embedded by dynamical travel time distributions). In the case of the random sampling scheme (which gives the same preference to all particles in storage, regardless of their ages to be sampled by discharge), TTD conditioned on a given time t, $p(t_T, t)$, coincides with the residence time distribution conditioned on the same time and is expressed as

$$p(t_T, t) = \frac{P(t - t_T)}{S(t - t_T)} \exp\left(\int_{t-t_T}^{t} -\frac{P(u)}{S(u)} du\right). \tag{3}$$

If the master equation is first multiplied by t_R and then integrated between 0 and ∞, a first-order linear differential equation is derived for the time-variant MTT [*Porporato and Calabrese*, 2015] which can be solved analytically. The general solution (under the random sampling assumption) is

$$\mathrm{MTT}(t) = \exp\left\{-\int_0^t \frac{P(u)}{S(u)} du\right\} . \left[\mathrm{MTT}_0 + \int_0^t \exp\left\{\int_0^u \frac{P(z)}{S(z)} dz\right\} du\right]. \tag{4}$$

where MTT_0 is the MTT at the beginning of a simulation period set arbitrarily. Higher-order moments of the TTD, however, should be numerically computed from equation (3).

3. Results and Discussion

3.1. Biasedness of Mean Travel Time (MTT) to Aggregation of Spatial Heterogeneity

We first focus on the simplest case for illustration purposes: a two component model in which two IA_i with different β_i and $S_{i,\mathrm{ref}}$ mix. To introduce significant contrasting heterogeneity among the IA_i, β_i and $S_{i,\mathrm{ref}}$ are sampled from uniform distributions varying between (1–50) and (20–1000) mm, respectively, giving a wide

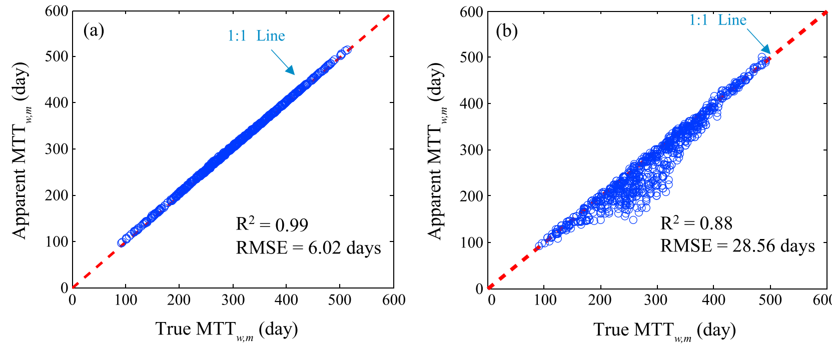

Figure 2. Effect of spatial heterogeneity on the scale of the aggregated time-variant travel time distribution (TTD). (a) Comparison of the apparent MTT (computed using the aggregated fluxes of the catchment and a time-varying lumped Langrangian formulation) with the true MTT (computed using the fluxes of the individual IAs) in a two reservoir system under the random sampling assumption. Each point corresponds to a catchment comprising of two IAs with contrasting MTTs. The excellent fit to the 1:1 line shows that the apparent MTTs estimated from the time-varying lumped stochastic Lagrangian formulation are unbiased as compared to the true MTTs which explicitly consider the spatial heterogeneity. (b) Apparent versus true MTT when the total storage in the mixture is calibrated by using simulated concentration time series in precipitation and streamflow (see Text S1 for details). These simulations demonstrate that the estimation of MTTs is still robust to aggregation of spatial heterogeneity when TTDs are constrained by concentration data.

range of system response to the input precipitation. For each IA, the hydrologic model is run over a 6 years period by using the daily precipitation data for the Redwood River Basin (44°33′N, 95°40′W), Minnesota, USA; however, one might use data from other locations or run a stochastic model to generate a synthetic precipitation time series. The resulting hydrologic fluxes (i.e., P, Q_i, and S_i) are then used in equation (3) (which assumes the random sampling scheme) to compute $p_i(t_T, t)$.

Under the aggregation of two IAs, the "true" TTDs in the mixture are computed by flow-weighted averaging of $p_i(t_T, t)$, $i = 1, 2$, to account for different mixing ratios arising from different instantaneous flows from each of the IA. Now if we pretend that we do not know the fluxes corresponding to the two IAs, but only know their aggregate flux (which would be the case in the absence of subcatchment data) and use this flux in equation (3), the "apparent" TTDs [after *Kirchner*, 2016a] can be obtained. In both cases, the marginal TTD, $p_{w,m}(t_T)$, representing the probability density that a given travel time can be observed during the simulation period, is estimated as

$$p_{w,m}(t_T) = \int_\Gamma p_w(t_T, \mathrm{t})\theta(t)dt. \qquad (5)$$

where Γ is the simulation period and the weights $\theta(t)$ are equal to the normalized discharge time series (by the total discharge over Γ) at the whole catchment outlet, from which the first moment denoted by $MTT_{w,m}$ is estimated. To avoid the influence of the arbitrary choice of the MTT_0, the first year of simulation is used as a warm-up period and the results for the last 5 years are reported and discussed.

Figure 2a shows the apparent versus true MTT for the case of a system with two spatially heterogeneous IAs under the random sampling assumption. The simulation was performed for 1000 pairs of IAs with MTTs differing by a factor of 1 to 5. The excellent coefficient of determination ($R^2 = 0.99$) and small root-mean-square error (RMSE = 6.02 days) shows that the apparent MTTs estimated from the time-varying lumped stochastic Lagrangian formulation of transport are unbiased as compared to the true MTTs which explicitly consider the spatial heterogeneity. This is because the influence of the IAs' spatial heterogeneity is translated into the time variability of the corresponding hydrologic fluxes (via the discharge-storage relationships), which is subsequently projected into the temporal dynamics of the combined fluxes of the IAs, used to compute the whole catchment's TTD. We additionally examined the aggregation error when the total storage in the mixture is not assumed known, but instead is calibrated using the simulated concentration time series of precipitation and streamflow (see Text S1 in the supporting information for details). Figure 2b demonstrates that the estimation of MTTs is still robust to aggregation of spatial heterogeneity when TTDs are constrained by the concentration data.

We also explored the biasedness of the apparent MTT to the aggregation of spatial heterogeneity if other than random sampling mechanisms were used (see Text S2). This was examined by assuming that the IAs and their mixture follow the same sampling scheme, giving high preference to water particles with younger ages while they are sampled as discharge from storage, under the same other simulation conditions used in Figure 2a (preference to younger ages has been revealed by many experimental and modeling studies [e.g., *Benettin et al.*, 2015a]). The results show that the relationship between the apparent and true MTTs is more scattered but not strongly biased as evidenced by R^2 = 0.88 and RMSE = 18.02 days (see Figure S1 in the supporting information). Further analysis (see Text S3 and Figure S2) reveals that under the random sampling assumption, the mixture's true sampling scheme tends to remain almost uniform, making thus the assumption of uniform sampling for the mixture reasonable. Nevertheless, this does not necessarily hold for other sampling schemes; i.e., the mixture's true sampling scheme might be significantly different from that assumed for the individual IAs. This implies that the scatter in Figure S1 might be partially attributed to the assumption that the mixture has the same sampling scheme as the individual IAs. Therefore, if one can determine or closely approximate the underlying sampling mechanism at some aggregation scale (e.g., from concentration time series), the apparent MTTs at that scale are expected to show even less scatter than that shown in Figure S1.

These observations are noteworthy for the following reasons. First, since climatic and stream hydrochemistry measurements are often only available at the whole catchment scale, the above findings indicate that the implemented time-variant lumped stochastic transport formulation can make use of such data to provide a reliable estimation of the MTT at some aggregated scale without needing to explicitly define the spatial heterogeneity at smaller scale, but still reflecting its influence. Although it was recently concluded that there is little basis for optimism that the MTT estimated from the existing methods is immune to aggregation error [*Kirchner*, 2016a, 2016b], our study provides a benchmark testing of the stochastic Lagrangian framework, demonstrating that its time-variant nature yields MTTs that are not significantly biased to the aggregation of spatial heterogeneity (e.g., compare Figure 2 with Figure 7 in *Kirchner* [2016a]). Second, our analysis highlights the advantage of this framework to estimate less biased MTTs as opposed to the extensively used sine-wave fitting method [e.g., *Soulsby et al.*, 2000; *Rodgers et al.*, 2005, among others]. *Kirchner* [2016a] elegantly showed that MTTs estimated by using the seasonal tracer cycles of precipitation and streamflow at the whole catchment scale via the sine-wave fitting method can be 6 times smaller than the true MTTs.

3.2. Variability of Mean Travel Time (MTT) Versus Scale of Spatial Aggregation

The numerical experiment presented above was extended to study the aggregation effect on TTD of a wider range of spatial variability and structured heterogeneity in the catchment organization. We first generate a TSS tree with a = 1.1, c = 2, and Ω = 5. Each channel is assigned a drainage area DA_i, randomly sampled from an exponential distribution with mean 3 km^2. The hydrologic model is then run to obtain the hydrologic fluxes at the outlet of each IA_i, and the outflows from all IA_i are routed through the river network by using the channels' topographic and geometric attributes (i.e., l_i, g_i, and b_i) determined as described in section 2.1. The flow routing scheme we used is based on the numerical solution of the coupled mass and momentum conservation equations for each channel (see *Mantilla et al.* [2006] for more details). Travel time analysis (using equation (4)) is then performed for all catchments with $1 \leq \Omega \leq 5$ but by using the routed fluxes at their corresponding outlets. We also assume that the transport time scales in the river channels are much smaller than those in the soil storage and are thus neglected.

The hierarchical aggregation of the IAs is found to reduce the variability in the MTTs, making them progressively less dependent on the network structured spatial heterogeneity. Moreover, as the aggregation scale increases, there exists a characteristic spatial scale (A^*) above which the variability in the MTT vanishes and the magnitude of MTT is not influenced by the aggregation of spatial heterogeneity. This is seen from Figure 3a which shows the $MTT_{w,m}$ versus the upstream area A_w, and Figure 3b in which A_w is in a logarithmic scale to make the scatter at the small spatial scales more visible. This observation raises the immediate question: what controls the magnitude of A^*?

To answer this question, numerous realizations of heterogeneous catchments were generated composed of exponentially distributed IAs with λ = 3 km^2 attached to branching structures corresponding to the generated TSS trees of parameters a = 1.1 and c = 2. Although TSS trees with the same a and c have the same probabilistic branching structure, each realization gives a river network exhibiting different channel connectivity as well as spatial arrangement of incremental areas. For each simulation, the variance of the MTTs over

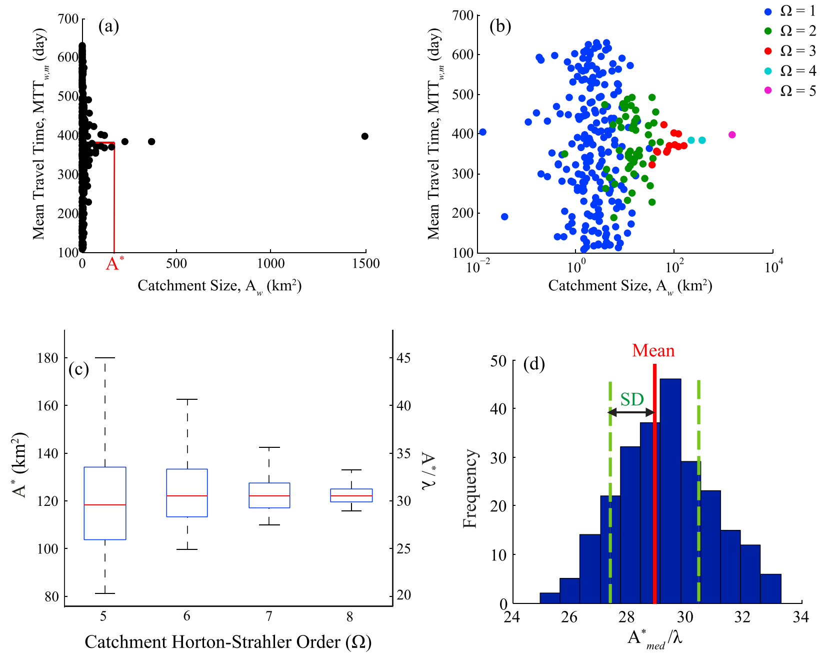

Figure 3. Emergence of a characteristic scale (A^*) at which the aggregation effects of spatial heterogeneity vanish. (a) Variability of catchment $MTT_{w,m}$ with the catchment size A_w in a fifth-order catchment composing of nested subcatchments. The catchment was synthetically generated by the Tokunaga model with parameters $a = 1.1$ and $c = 2$ and IAs with an exponential distribution with mean $\lambda = 3$ km^2. As the hierarchical aggregation of IAs takes place, $MTT_{w,m}$ shows a convergence to a constant value after A^*. (b) The same plot as Figure 3a, but the horizontal axis is in a logarithmic scale so that the scatter at the small spatial scales is more visible. Catchments with the same Horton-Strahler order (Ω) are also depicted by distinct colors. (c) A^* versus Ω for 1000 realizations of Tokunaga trees with $a = 1.1$, $c = 2$, $\lambda = 3$ km^2, and Ω = 5, 6, 7, and 8. For each realization, DA_i and β_i were randomly sampled from exponential distribution with mean λ and uniform distribution spanning the ranges of 1–50, respectively. The right axis shows A^*/λ versus Ω. The median of A^*/λ, i.e., A^*_{med}/λ, takes place at almost the same magnitude in catchments with different orders, while its variance decreases as the catchment's order increases. (d) Histogram of the ratio A^*_{med}/λ for the Tokunaga trees with Ω = 5, and parameters a and c ranging in [0.9–1.3] and [2–3.4], respectively (1000 simulations per each pair of a and c). A^*_{med}/λ is seen to vary between 25.0 to 33.3 with mean 29.2 and standard deviation of 1.7, suggesting that A^*_{med}/λ does not depend significantly on the river networks' probabilistic branching structure.

increasing spatial scales is computed and A^* is identified as the scale after which the standard deviation of MTTs is less than 0.01 day. The variability of A^* across four sets of simulations, each including 1000 realizations of TSS trees with Ω = 5, 6, 7, and 8, shows that regardless of the catchment's order (or size), the median of A^* (denoted by A^*_{med} from here on) takes place at almost the same magnitude (Figure 3c), implying independence to the catchment's underlying river network topology and the spatial arrangement of the IAs within a catchment. Also, the variance of A^* is seen to decrease as the catchment's order increases because in higher-order catchments, there exists a larger number of lower order branchings that aggregate, hence their heterogeneity imposes less influence on the overall variability of MTT.

The magnitude of A^*_{med} obtained from these experiments is ~120 km^2 (see Figure 3c). However, this is not a universal value and it relates to the catchment mean incremental area (λ) and the channel initiation area (A_0), which were kept constant in the above numerical experiments. For instance, if two catchments with the same total drainage area are considered, the one with smaller A_0 would be dissected by a larger number of channels (or IAs), resulting in larger drainage density, smaller λ, and hence smaller A^*. Since both A^* and λ vary with A_0 in the same direction, their ratio might not depend on A_0. We examine this by extracting multiple river networks from 10 m digital elevation model of the Redwood River Basin by defining different A_0 ranging from 0.05 to 0.5 km^2 [e.g., *Tarboton et al.*, 1991], and the corresponding λ were computed by delineating the IAs of each channel network (we note that switching from synthetic to real river networks for this experiment was simply because A_0 cannot be introduced while generating TSS trees). By repeating the travel time analysis on the extracted networks, Figure S3 shows that A^*_{med}/λ does not change significantly with A_0, spanning from 25.9 to 33.4 with mean 28.7 and standard deviation of 2.4 (see also Figure S4 for the relationship between A^*_{med}, A_0, and drainage density, as well as the illustration on the independence of $A^*_{\mathrm{med}}/\lambda$ to the catchment drainage density). Accordingly, Figure 3c was transformed by plotting A^*/λ versus Ω (right y axis), indicating that $A^*_{\mathrm{med}}/\lambda$ varies slightly between 28.87 and 29.54 with mean 29.2 and standard deviation of 0.45.

3.3. Dependence of Catchment Characteristic Scale on Tokunaga Parameters

Since the estimation of the TSS parameters for a catchment is robust to the A_0 used to define the first-order channels [*Zanardo et al.*, 2013], we further examine the dependence of $A^*_{\mathrm{med}}/\lambda$ to the Tokunaga parameters a and c. Figure 3d shows the histogram of $A^*_{\mathrm{med}}/\lambda$ for the TSS trees with $\Omega = 5$ and parameters a and c ranging in [0.9–1.3] and [2–3.4], respectively (1000 simulations per each pair of a and c). The chosen Tokunaga parameters are within the range reported by *Zanardo et al.* [2013, Figure 9] for the majority of the river basins across the United States. For all values of the Tokunaga a parameter, significant negative correlation was found between $A^*_{\mathrm{med}}/\lambda$ and the c parameter (Pearson's linear correlation coefficient > -0.8 and P-value < 0.003 at 5% significant level). This is because in a river network with a larger value of c, there exists a larger number of low-order channels merging to higher-order branches; hence, the characteristic scale emerges at smaller spatial scales as a larger number of low-order channels is available for aggregation to reach the characteristic scale faster. Nevertheless, for all combinations of a and c, $A^*_{\mathrm{med}}/\lambda$ is seen to change between 25.0 to 33.3 with mean 29.2 and standard deviation of 1.7, suggesting that $A^*_{\mathrm{med}}/\lambda$ does not depend significantly on the river networks' probabilistic branching structures. Indeed, from the simulation results it turns out that there exists a level of hierarchy in catchments at which the spatial heterogeneity loses its dominance on the MTT (which is the direct consequence of the central limit theorem) and the magnitude of such a characteristic spatial scale in high-order catchments is on average approximately equal to 30 times the mean incremental area.

The above findings have practical implications pertaining to data measurements in the field and inferences that can be made on transport time scales and mixing processes across spatial scales. Specifically, if the interest is to understand the functioning of a large catchment, collecting data at scales smaller than A^* does not allow extrapolation to estimate the MTT at larger scales. However, the MTT estimated via a time-variant Lagrangian transport formulation and for scales comparable to A^* is not significantly influenced by aggregation effects, allowing thus reliable interpretation and inference at the catchment scale.

4. Conclusions

The absence of rigorous data and theories for extrapolating information from the field to the larger scales [e.g., *Hrachowitz et al.*, 2013] necessitates developing reduced-complexity frameworks that are still able to explain the spatial heterogeneity and process complexity in real-world catchments [*McDonnell et al.*, 2007; *Troch et al.*, 2009]. In this study, we examined the ability of the lumped stochastic Lagrangian formulation for water and solute transport in providing reliable estimates of the mean travel time (MTT) in spatially heterogeneous catchments. Via numerical simulations of heterogeneous catchments, we showed that a time-varying travel time distribution (TTD) formulation results in MTTs that are not significantly biased to the aggregation of spatial heterogeneity under different age sampling assumptions. This finding reinforces the importance of such a time-variant lumped formalism to appropriately predict the catchment's mean transport time scales without the need to explicitly characterize and embed the small-scale spatial heterogeneity. Although significant variability of MTT exists at small spatial scales, there exists a characteristic spatial scale (A^*) above which the MTT converges to a constant value not influenced by the aggregation of spatial heterogeneity. This observation is a direct consequence of the central limit theorem regardless of the method being used to estimate the MTT. However, time-variant versus time-invariant methods can result in significantly different MTT estimates at large catchment scales and our results speak for the advantage of using a time-variant formulation for obtaining unbiased estimates. The ratio between the characteristic scale A^* and the mean incremental area was also shown to be on average independent of the river network topology and spatial arrangement of incremental areas.

This work is one small step toward understanding the dependence of MTT on the network-structured spatial heterogeneity, and further study is required to explore the impact of other catchment physical characteristics (such as hillslope gradient, aspect, soil depth to groundwater, subsurface flow path length, and proportion of hydrologically responsive soil) on the MTT at hierarchical spatial scales. While the focus here was only on the MTT, extension of our analysis to the aggregation bias of the whole TTD is feasible and this would allow to quantify the ability of the time-variant Lagrangian transport formulation to accurately estimate lower quantiles of the distribution, an important issue in real-world applications in view of the short-time sampling horizons on which longer-term inferences are to be made.

Acknowledgments
This research was funded by NSF grant EAR-1209402 under the Water Sustainability and Climate Program (WSC): REACH (REsilience under Accelerated CHange) and benefited from collaborations made possible by NSF grants EAR-1242458 (LIFE: Linked Institutions for Future Earth) and EAR-1342944.

References

Benettin, P., Y. van der Velde, S. E. A. T. M. van der Zee, A. Rinaldo, and G. Botter (2013a), Chloride circulation in a lowland catchment and the formulation of transport by travel time distributions: Chlorides catchment transport, *Water Resour. Res.*, *49*, 4619–4632, doi:10.1002/wrcr.20309.

Benettin, P., A. Rinaldo, and G. Botter (2013b), Kinematics of age mixing in advection-dispersion models, *Water Resour. Res.*, *49*, 8539–8551, doi:10.1002/2013WR014708.

Benettin, P., J. W. Kirchner, A. Rinaldo, and G. Botter (2015a), Modeling chloride transport using travel time distributions at Plynlimon, Wales, *Water Resour. Res.*, *51*, 3259–3276, doi:10.1002/2014WR016600.

Benettin, P., A. Rinaldo, and G. Botter (2015b), Tracking residence times in hydrological systems: Forward and backward formulations: Forward and backward TTD, *Hydrol. Process.*, *29*(25), 5203–5213.

Birkel, C., and C. Soulsby (2015), Advancing tracer-aided rainfall-runoff modelling: A review of progress, problems and unrealised potential: Advancing tracer-aided rainfall-runoff modelling, *Hydrol. Process.*, *29*(25), 5227–5240.

Botter, G., E. Milan, E. Bertuzzo, S. Zanardo, M. Marani, and A. Rinaldo (2009), Inferences from catchment-scale tracer circulation experiments, *J. Hydrol.*, *369*(3–4), 368–380, doi:10.1016/j.jhydrol.2009.02.012.

Botter, G., E. Bertuzzo, and A. Rinaldo (2010), Transport in the hydrologic response: Travel time distributions, soil moisture dynamics, and the old water paradox, *Water Resour. Res.*, *46*(3), doi:10.1029/2009WR008371.

Botter, G., E. Bertuzzo, and A. Rinaldo (2011), Catchment residence and travel time distributions: The master equation, *Geophys. Res. Lett.*, *38*, L11403, doi:10.1029/2011GL047666.

Danesh-Yazdi, M., E. Foufoula-Georgiou, D. L. Karwan, and G. Botter (2016), Inferring changes in water cycle dynamics of intensively managed landscapes via the theory of time-variant travel time distributions, *Water Resour. Res.*, *52*, 7593–7614, doi:10.1002/2016WR019091.

Ginn, T. R. (1999), On the distribution of multicomponent mixtures over generalized exposure time in subsurface flow and reactive transport: Foundations, and formulations for groundwater age, chemical heterogeneity, and biodegradation, *Water Resour. Res.*, *35*(5), 1395–1407, doi:10.1029/1999WR900013.

Hack, J. T. (1957), Studies of longitudinal stream profiles in Virginia and Maryland, *U.S. Geol. Surv. Prof. Pap.*, *294-B*, 1–97.

Harman, C. J. (2015), Time-variable transit time distributions and transport: Theory and application to storage-dependent transport of chloride in a watershed, *Water Resour. Res.*, *51*, 1–30, doi:10.1002/2014WR015707.

Hornberger, G. M., T. M. Scanlon, and J. P. Raffensperger (2001), Modelling transport of dissolved silica in a forested headwater catchment: The effect of hydrological and chemical time scales on hysteresis in the concentration-discharge relationship, *Hydrol. Process.*, *15*, 2029–2038.

Hrachowitz, M., et al. (2013), A decade of predictions in ungauged basins (PUB)—A review, *Hydrol. Sci. J.*, *58*(6), 1198–1255.

Kirchner, J. W. (2006), Getting the right answers for the right reasons: Linking measurements, analyses, and models to advance the science of hydrology, *Water Resour. Res.*, *42*, W03S04, doi:10.1029/2005WR004362.

Kirchner, J. W. (2016a), Aggregation in environmental systems—Part 1: Seasonal tracer cycles quantify young water fractions, but not mean transit times, in spatially heterogeneous catchments, *Hydrol. Earth Syst. Sci.*, *20*(1), 279–297.

Kirchner, J. W. (2016b), Aggregation in environmental systems—Part 2: Catchment mean transit times and young water fractions under hydrologic nonstationarity, *Hydrol. Earth Syst. Sci.*, *20*(1), 299–328.

Mantilla, R., V. K. Gupta, and O. J. Mesa (2006), Role of coupled flow dynamics and real network structures on Hortonian scaling of peak flows, *J. Hydrol.*, *322*(1–4), 155–167, doi:10.1016/j.jhydrol.2005.03.022.

McDonnell, J. J., et al. (2007), Moving beyond heterogeneity and process complexity: A new vision for watershed hydrology, *Water Resour. Res.*, *43*, W07301, doi:10.1029/2006WR005467.

McGuire, K. J., and J. J. McDonnell (2006), A review and evaluation of catchment transit time modeling, *J. Hydrol.*, *330*(3–4), 543–563.

Peckham, S. D. (1995a), New results for self-similar trees with applications to river networks, *Water Resour. Res.*, *31*(4), 1023–1029, doi:10.1029/94WR03155.

Peckham, S. D. (1995b), Self-similarity in the three-dimensional geometry and dynamics of large river basins, PhD thesis, Univ. of Colo., Boulder.

Porporato, A., and S. Calabrese (2015), On the probabilistic structure of water age, *Water Resour. Res.*, *51*, 3588–3600, doi:10.1002/2015WR017027.

Rinaldo, A., K. J. Beven, E. Bertuzzo, L. Nicotina, J. Davies, A. Fiori, D. Russo, and G. Botter (2011), Catchment travel time distributions and water flow in soils: Catchment travel times, *Water Resour. Res.*, *47*, W07537, doi:10.1029/2011WR010478.

Risken, H. (1984), Fokker-Planck equation, in *The Fokker-Planck Equation*, vol. 18, pp. 63–95, Springer, Berlin.

Rodgers, P., C. Soulsby, S. Waldron, and D. Tetzlaff (2005), Using stable isotope tracers to assess hydrological flow paths, residence times and landscape influences in a nested mesoscale catchment, *Hydrol. Earth Syst. Sci.*, *9*(3), 139–155, doi:10.5194/hess-9-139-2005.

Rodríguez-Iturbe, I., and A. Rinaldo (2001), *Fractal River Basins: Chance and Self-organization*, 558 pp., Cambridge Univ. Press.

Sanford, W. E., and J. P. Pope (2013), Quantifying groundwater's role in delaying improvements to Chesapeake Bay water quality, *Environ. Sci. Technol.*, *47*(23), 13330–13338.

Soulsby, C., R. Malcolm, R. Helliwell, R. C. Ferrier, and A. Jenkins (2000), Isotope hydrology of the Allt a' Mharcaidh catchment, Cairngorms, Scotland: Implications for hydrological pathways and residence times, *Hydrol. Process.*, *14*(4), 747–762, doi:10.1002/(SICI)1099-1085(200003)14:4<747::AID-HYP970>3.0.CO;2-0.

Soulsby, C., D. Tetzlaff, and M. Hrachowitz (2009), Tracers and transit times: Windows for viewing catchment scale storage?, *Hydrol. Process.*, *23*(24), 3503–3507, doi:10.1002/hyp.7501.

Tarboton, D. G., R. L. Bras, and I. Rodriguez-Iturbe (1991), On the extraction of channel networks from digital elevation data, *Hydrol. Process.*, *5*(1), 81–100, doi:10.1002/hyp.3360050107.

Troch, P. A., G. A. Carrillo, I. Heidbüchel, S. Rajagopal, M. Switanek, T. H. M. Volkmann, and M. Yaeger (2009), Dealing with landscape heterogeneity in watershed hydrology: A review of recent progress toward new hydrological theory, *Geogr. Compass*, *3*(1), 375–392.
van der Velde, Y., P. J. J. F. Torfs, S. E. A. T. M. van der Zee, and R. Uijlenhoet (2012), Quantifying catchment-scale mixing and its effect on time-varying travel time distributions, *Water Resour. Res.*, *48*, W06536, doi:10.1029/2011WR011310.
Woo, D. K., and P. Kumar (2016), Mean age distribution of inorganic soil-nitrogen, *Water Resour. Res.*, *52*, 5516–5536, doi:10.1002/2015WR017799.
Young, P. (2003), Top-down and data-based mechanistic modelling of rainfall-flow dynamics at the catchment scale, *Hydrol. Process.*, *17*(11), 2195–2217.
Zanardo, S., I. Zaliapin, and E. Foufoula-Georgiou (2013), Are American rivers Tokunaga self-similar? New results on fluvial network topology and its climatic dependence, *J. Geophys. Res. Earth Surf.*, *118*, 166–183, doi:10.1029/2012JF002392.